Biosensors and Bioelectronics 137 (2019) 207–212

Contents lists available at ScienceDirect

Biosensors and Bioelectronics

journal homepage: www.elsevier.com/locate/bios

Single conical track-etched nanopore for a free-label detection of OSCS contaminants in heparin

Tianji Ma[a], Emmanuel Balanzat[b], Jean-Marc Janot[a], Sébastien Balme[a,*]

[a] Institut Européen des Membranes, UMR5635 UM ENSCM CNRS, Place Eugène Bataillon, 34095, Montpellier Cedex 5, France
[b] Centre de recherche sur les Ions, les Matériaux et la Photonique, UMR6252 CEA-CNRS-ENSICAEN, 6 Boulevard du Maréchal Juin, 14050, Caen Cedex 4, France

ARTICLE INFO

Keywords:
Nanopore
Heparin
OSCS
Track-etched

ABSTRACT

The heparin contamination by oversulfated chondroitin (OSCS) was at the origin of one major sanitary problem of last decade. Here we propose a novel strategy to detect OSCS from heparin solution based on conical nanopore functionalized with poly-L-lysine deposition to ensure its re-usability. This sensor is an excellent to detect low heparin concentration (from 25 ng/ml to 3 μg/ml) using the modification of ionic current rectification. It also allows following the kinetic of heparin degradation by heparinase with a good correlation with results obtained by classical methods. The sensor is sensitive to the inhibition of heparinase by OSCS until a concentration of 200 pg/ml representing 0.01% in weight in a heparin. This resolution is one order of magnitude lower than the one obtained by chromatography. For the first time, it was reached without fluorescence labeling.

1. Introduction

Heparin (HEP) is a commonly used as anticoagulant to treat several clotting disorders. 10 years ago, a sanitary problem from contamination of oversulfated chondroitin (OSCS) has caused the death of about 200 patients around the world (Guerrini et al., 2009; Sasisekharan and Shriver, 2009). Since this event, an effort was made to detect small amount of OSCS from heparin mixture that is not easy due to their close structures (Beni et al., 2011). To this end, the classical methods based on chromatography were the first considered. However they are limited to a detection limit around 0.3% in weight and required expensive instruments such as mass spectrometer or NMR to identify the OSCS(Liu et al., 2011). More recently, the fluorescence based sensors allow to improve the detection limit until from 10^{-2}% until 10^{-9}% weight (Kalita et al., 2014). The OSCS detection is usually indirect since they used ability to inhibit the HEP degradation by heparinase. Despite their low detection limits, the major weakness of these fluorescence sensors is that they require fluorescent probes (Ding et al., 2015; Wang et al., 2016), nanoparticles (Kalita et al., 2014) and/or biomolecules (Hu et al., 2016) engineering for the specific detection of heparin as well as fluorescence spectrometer microscope equipment. Thus provide a simple and cheap technology to detect OSCS from HEP sample is still highly challenging.

The single nanopore is versatile method for macromolecule sensing that emerged last two decades (Dekker, 2007; Kasianowicz et al., 1996). Using the resistive pulse technique through solid-state nanopore, a sample of HEP contaminated by OSCS can be identified (Karawdeniya et al., 2018). However, the concentration cannot be obtained by this way. In addition, the major problems of solid-state nanopore are the short lifetime and the low success rate of experiments which limit the real application, despite recent improvements by PEG functionalization (Giamblanco et al., 2018b; Roman et al., 2018, 2017). The conical track-etched nanopore is a good alternative to design label-free sensor based on the modulation of ionic current rectification (ICR)(Lepoitevin et al., 2017, 2016a). Based on that, small molecules as well as proteins can be specifically detected by a ligand/receptor systems (Ali et al., 2016, 2015, 2010a; 2010b). However, these sensors are often one-off especially when the ligand binding is not totally reversible. Recently, we have shown that the reversible functionalization with poly-L-lysine (PLL) could be promised for biosensing applications (Lepoitevin et al., 2016b). Another, advantage to use polyelectrolytes (PE) inside nanopore is that the layer-by-layer deposition can be monitored and the kinetic depends on their properties (size and charge) (Ma et al., 2018). Following our previous investigations in this field, we propose here to design a reusable sensor for OSCS contained in a HEP sample. Our strategy is based on (i) the reversibility of PLL/HEP functionalization of a conical nanopore and (ii) the degradation of the HEP by heparinase which is inhibited by the OSCS. Here, we assume that action of enzyme will decrease the affinity between degraded HEP and the PLL. This would impact the nanopore surface charge and thus the ICR.

* Corresponding author.
E-mail address: sebastien.balme@univ-montp2.fr (S. Balme).

https://doi.org/10.1016/j.bios.2019.05.005
Received 7 March 2019; Received in revised form 1 May 2019; Accepted 3 May 2019
Available online 07 May 2019
0956-5663/

In order to prove the concept that conical nanopore could be a suitable alternative to detect the HEP contamination by OSCS, we present our work in several following steps. First, we will demonstrate the reversibility of the PLL/HEP deposition as well as their impact on the IRC. Then, we will evaluate the impact of the HEP concentration on the IRC in order to evidence a dose-response curve. The OSCS contained in HEP solution will be detected using heparinase. Thus, we will follow the kinetic of degradation of HEP by heparinase by nanopore and compared the results with a classical method. Then, using this strategy, we will study the relationship OSCS concentration ICR to establish the dose-response dependence. The last sections will be dedicated to discuss the reproducibility of sensing experiments and the nanopore sensor lifetime. This last step will aim to validate our sensor.

2. Material and methods

2.1. Material

Poly(ethylene-terephthalate) (PET) film (thickness 13 µm, biaxial orientation) was purchased from Goodfellow (ES301061). Sodium chloride (71380), potassium chloride (P3911), sodium hydroxide (30603), hydrogen chloride (30721), trizma hydrochloride (T3253), CAPS (C2632), sodium acetate (W302406), ethylenediaminetetraacetic acid (EDTA) (E5513), Poly-L-lysine hydrobromide (PLL) (30 kD-70kD P2636), Heparin sodium salt from porcine intestinal mucosa (HEPep) (H4784), Heparinase I and III Blend from Flavobacterium heparinum (H3917), Heparinase II from Flavobacterium heparinum (H6512) were purchased from Sigma-Aldrich. Over Sulfated Chondroitin Sulfate (OSCS) Standard (3125401) was purchased from SERVA. Ultra-pure water was produced from a Q-grad®-1 Milli-Q system (Millipore).

2.2. Track-etching nanopores and current –voltage measurements

The PET films (13 µm) were irradiated by a single Xe irradiation (8.98 MeV) (GANIL, SEM line, Caen, France) to create single tracks and thus a single nanopore. Then, the latter was exposed to UV irradiation during 9 h for tip side and 15 h for base side (Fisher bioblock; VL215.MC, λ = 302 nm). The activated PET film was mounted between two chambers of a Teflon cell. The etchant solution (NaOH 9 M, 1.6 ml) was added on the base side and the stopping solution (KCl 1M and CH3COOH 1M, 1.6 ml) on the tip side. An electrode (Pt) is immersed in the stop solution and the working one (Pt) in the etchant solution and then a potential of 1 V was applied across the membrane. The nanopore opening was characterized by the current as a function of time recorded by a patch-clamp amplifier (EPC-10 HEKA electronics, Germany). The etching process was stopped by replacement of the etching solution by the stop one when the current reach a value of several hundred pA.

The tip diameter d of the conical nanopore was determined from the dependence of the conductance G measured in the linear zone of the I–V curve (typically between - 60 mV and 60 mV) assuming a bulk-like ionic conductivity inside the nanopores (equation (1)).

$$G = \frac{\kappa d D \pi}{4L} \quad (1)$$

Where, κ is the ionic conductivity of the solution, L is the nanopore length (13 µm) and D is based diameter which was calculated from the total etching time t using the relationship $D = 2.5t$ (the factor 2.5 was determined in our experimental set up using multipore track-etched membranes).

The I–V curve were obtained from the current traces recorded as a function of time from 1 V to −1 V by 100 mV steps for 2 s and from 100 mV to −100 mV by 10 mV steps for 2s using a sampling rate 50 kHz.

2.3. Nanopore functionalization and reversibility of PLL/HEP layer

The same buffer solution (50 mM Tris-HCl, 75 mM CH_3COONa, 100 mM NaCl) was used for polyelectrolyte adsorption and enzymatic degradation. The pH is adjusted to 7.5 by addition of chloride acid and sodium hydroxide. For the functionalization with PLL, 10 µl of the polyelectrolyte solution (1 mg/ml) was added in the tip side of the nanopore. A voltage -1V was applied from the tip side to the base one during 3 min. Then a various volume of HEP (1 mg/ml) was added in 1.6 ml buffer solution at tip side of the cell. The 1 V for HEP was applied for 3 min. The I–V curves were recorded after replacing polyelectrolyte solution by buffer. After each detection of HEP, the PLL-HEP layer was desorbed using a buffer at pH 12 containing 100 mM KCl, 5 mM Trizma-HCl and 1 mM EDTA.

2.4. Enzymatic degradation

50 U of Heparinase I and III was dissolved in 2.5 ml of storage solution containing 20 mM Tris-HCl, 100 mM NaCl, 1 mM EDTA at pH 7.5. 10 U of Heparinase II is dissolved in 1 ml of the same buffer. 0.25 ml of Heparinase I and III at 20 U/ml and 0.5 ml off Heparinase II at 10 U/ml are mixed and then diluted 10 times. So the final solution has a concentration of 1.33 U/ml of total enzyme.

The enzymatic reaction is carried out at ambient temperature ~25 °C during time from 0 to 250 min in the buffer solution pH 7.5 containing 50 mM Tris-HCl, 75 mM (CH3COO)Na, 100 mM NaCl. For each essay, 3 µl of HEP (1 mg/ml) and 5 µl of enzyme cocktail solution (1.33 U/ml) are added in 1.5 ml of the reaction buffer solution. So the concentrations of HEP and Heparinase for reaction are 2 µg/ml and 4.43 mU/ml respectively.

For OSCS detection, 2 mg OSCS is dissolved in 20 ml storage solution described above. Then 1 ml of this solution is dissolved by 10 times (10 µg/ml) and 1 ml dissolved by 1000 times (0.1 µg/ml). To obtained the OSCS/heparin ratio 10%, 1%, 0.1%, 0.01% w/w, 30 µl, 3 µl of OSCS (10 µg/ml) or 30 µl, 3 µl of OSCS (0.1 µg/ml) was added in 1.5 ml of reaction solution containing HEP at 2 µg/ml. Then 4.43 mU/ml of enzyme solution was added. The enzymatic reaction was carried out at 25 °C during 200 min.

3. Results and discussions

The strategy to obtain the nanopore sensor is illustrated on Fig. 1. It consists to open a single conical nanopore on a PET film and decorated it by adsorption of PLL. Then, as mention in introduction, our methodology has follow three steps of detection (i) the HEP (ii) the HEP degraded by heparinase and (iii) the HEP degraded by heparinase in presence of OSCS.

3.1. Heparin detection by conical nanopore decorated with PLL

The PET single conical nanopores were obtained by track-etched methods under dissymmetrical condition as previously described (Lepoitevin et al., 2015). Shortly, we used the electrostopping method. The D_{base} is deduced from the etching time. In order to confirm the factor used is suitable and evaluate the impact of the dispersity of the base diameter, we performed the same experiment on low density membrane (10^5 pores/cm$^{2)}$ to avoid the nanopores overlap. In Fig. S1 are reported the SEM of several nanopores obtained after etching time 156 min. From the etching time and conductance measured on a single nanopore performed in the same condition, we obtained a D_{base} = 390 nm and a d_{tip} = 22.5 nm. Accoring to the dispersity observed on the multipore membrane (Fig. S1) the error on the d_{tip} about 1.5 nm. After alkaline etching, the nanopore inner wall exhibits carboxylate moieties which confer it a negative surface charge. The I–V dependence recorded at pH 7 NaCl 100 mM shows ICR behavior characterized by the rectification factor $Rf = |I\ (1V)/I\ (-1V)| < 1$

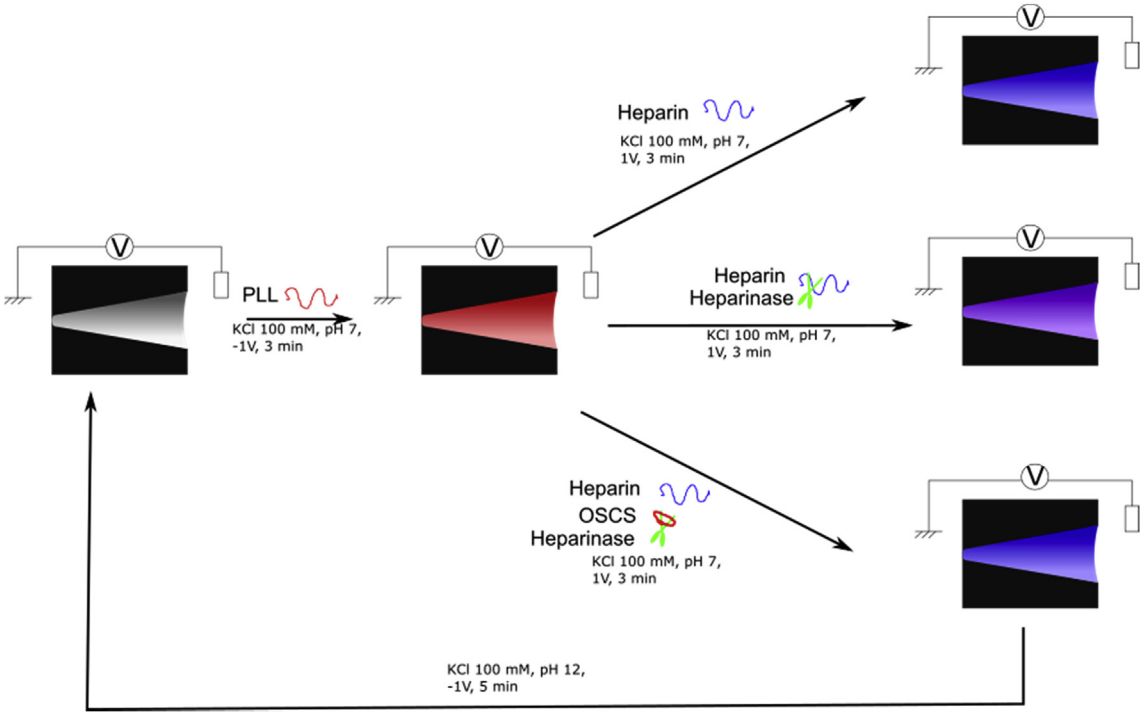

Fig. 1. Sketch of experimental methodology follows in this work. The first step is the nanopore functionalization by PLL. The second step is the different experiments performed to detect HEP and OSCS.

(Fig. 2). The first set of experiment is dedicated to show the nanopore functionalization by PLL and the HEP detection. To do so, the PLL was added in the tip chamber and a voltage −1 V was applied until inversion of I–V curve that is characteristic to the inversion of the nanopore surface charge (Figs. 2 and S2). After washing, the heparin was added to the tip chamber under 1 V during 3 min.

The I–V curve was again inversed due to the excess of negative charge from heparin. This evidences that each polyectrolyte can be detected by the conical nanopore. The first targeted property of our nanopore sensor is its reusability. To prove that, we have performed several cycles of PLL/HEP adsorption followed by a washing at pH 12 under 1V during 5 min to remove the PE layers on different nanopores with similar size. The *Rf* as well as the conductance recorded after each step are similar for the 18 cycles (Fig. 2 and S3) and 4 cycles (Fig. S4). This confirms as expected that conical nanopore is reusable for the heparin detection.

Our nanopore is suitable to detect HEP using the IRC. We have to demonstrate if the value of *Rf* is dependent on the HEP concentration in order to establish a dose-response curve. We can notice that at low concentration, the adsorption of PE onto a charged surface is usually described by a Langmuir model. Here, the detection method by ICR does not give the exact interfacial concentration of PE but it is sensitive to the modification of the global surface charge. We measured the I–V dependence after adsorption of HEP for different bulk concentrations following the cycle PLL/HEP adsorption and washing at pH 12 (Fig. 3). The rectification factor after each step for two consecutive quantitative analyses was reported on Fig. S4 to confirm the constant values after PLL adsorption and after washing. Conversely, the rectification factor

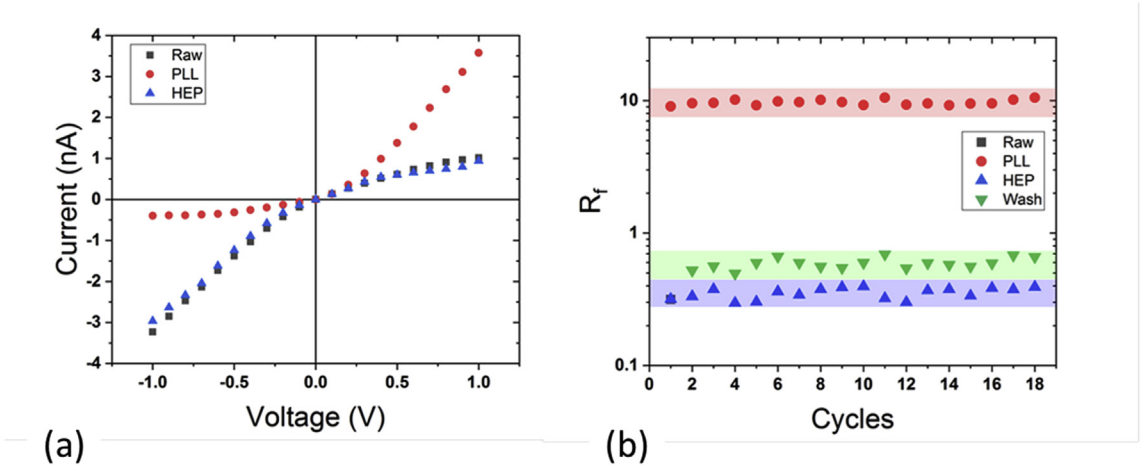

Fig. 2. (a) Sketch of experimental functionalization and heparin detection using conical nanopore, (a) I–V curve of raw single nanopore (black, square), after PLL deposition (red, circle) and after heparin deposition (blue, triangle), (b) Rectification factor obtained for raw single nanopore (black, square), after PLL deposition (red, circle), heparin deposition (blue, triangle) and washing at pH 12 (green triangle). The experiments were performed on a single nanopore d_{tip} = 22.5 nm and D_{base} = 390 nm. (For interpretation of the references to colour in this figure legend, the reader is referred to the Web version of this article.)

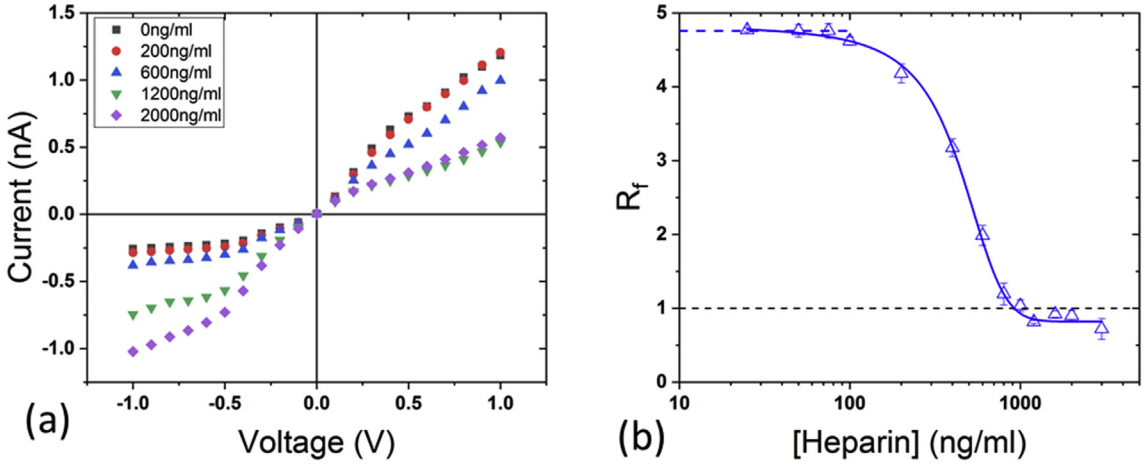

Fig. 3. (a) I–V dependence after HEP adsorption at different bulk concentrations (b) R_f as a function of HEP bulk concentration. The blue dash line corresponds to the R_f measured after PLL adsorption and the full line to non-linear fit by equation (1). The experiments were performed on a single nanopore d_{tip} = 35 nm and D_{base} = 300 nm for a total number of cycle n = 28. (For interpretation of the references to colour in this figure legend, the reader is referred to the Web version of this article.)

decreases with the heparin concentration in the bulk. This means that the positive charges of PLL are counterbalanced by the increase of HEP amount adsorbed inside the nanopore. Assuming that the HEP adsorption on PLL is mainly governed by the electrostatic interactions, the amine groups of PLL layer can be seen as binding sites for acidic moieties of the HEP. In this case the rectification factor can be assimilated to the bound fraction of HEP on PLL as following equilibrium.

$$[PLL] + [HEP] \rightleftarrows [PLL - HEP]$$

The plot of rectification factor as a function of HEP concentration in the bulk can be fitted by a classical sigmoidal equation (eq. (2)) equation where the asymptotic values are the rectification factor induced by only the PLL (Rf_{PLL}) and after saturation by HEP (Rf_{HEP}). The sigmoidal curve comes from the fact that to modify the IRC a sufficient amount of HEP has to be adsorbed to impact the nanopore surface charge. At low concentration, the amount of HEP adsorbed is not sufficient to significantly modify the nanopore surface charge and thus the IRC. In this case, the transport is mainly dominated by the PLL charge. With the increase of HEP concentration, more and more HEP are adsorbed and thus affect the IRC. In this range, the nanopore sensor is suitable to obtain the dose-response of HEP based on the *Rf*. Finally, when HEP concentration reaches a certain value the adsorption is very fast and the *Rf* become constant.

$$Rf = Rf_{PLL} + \frac{Rf_{HEP} - Rf_{PLL}}{1 + 10^{(logEC50 - c)p}} \quad (2)$$

where the half maximal effective concentration EC50 is the bulk concentration where HEP reaches 50% of PLL coverage, *c* the concentration of HEP in the solution and *p* the equivalent of Hill coefficient which gives information about degree of interaction between the binding sites of PLL and the HEP. The non-linear fit (Fig. 3b) gives an $EC50 = 435.9$ ng/ml and a $p = -2.79\ 10^{-3}$. The *p* value below 1 means that when a HEP is bound on PLL its affinity for another HEP molecule decrease. This result highlights that the HEP adsorption inside the nanopore should not be described by a Langmuir isotherm since this model assumes that binding sites are completely independent. This result opens numerous questions about our basic conception of polyelectrolyte adsorption under confinement that is crucial for the understanding the membrane functionalization using such macromolecules.

3.2. OSCS detection by conical nanopore decorated with PLL

Our concept for OSCS sensing is based on its ability to inhibit the HEP degradation by heparinase. As first step, we have to establish a correlation between the IRC and the degradation degree of HEP. To do so, we adsorbed the HEP after different degradation time by heparinase. As shown on Fig. 4, the rectification factor increases with the degradation time of HEP. This can be explained by a weaker affinity of oligosaccharide from the HEP with the PLL due to their lower molecular weight. The kinetic of HEP degradation obtained by nanopore experiment is compared with the one obtained by a classical method which consists of dose the oligosaccharide by absorbance at 214 nm (Fig. 4 and SI-6). It follows an order 1 kinetic law (eq. (3)).

$$[P] = [P_0]\exp(-kt) \quad (3)$$

where *P* is the product of Hep degradation. The value of kinetic constant *k* obtained by nanopore detection ($k = 1.12\ 10^{-2} \pm 0.6\ 10^{-2}$) and absorbance ($k = 1.56\ 10^{-2} \pm 0.06\ 10^{-2}$) are very close proving that the nanopore functionalized with PLL is a good candidate to follow easily the enzymatic degradation of PE. It could be noticed that using a single nanopore, the enzymatic degradation was only characterized by resistive pulse method (Fennouri et al., 2013; Giamblanco et al.,

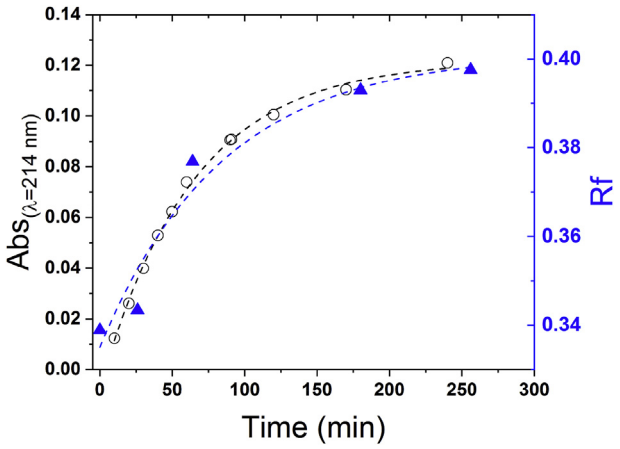

Fig. 4. Enzymatic degradation of HEP by heparinase follows by absorbance-based methods (black, circle) and nanopore functionalized by PLL. The experiments was performed on one nanopore d_{tip} = 29 nm and D_{base} = 340 nm following 5 cycles of PLL-HEP adsorption/washing at pH12.

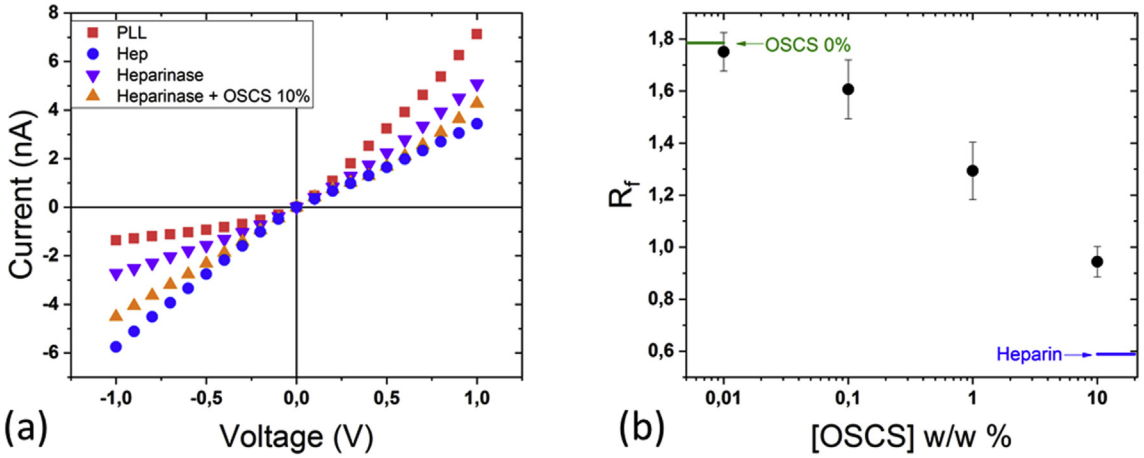

Fig. 5. (a) Sketch of the OSCS detection using single PLL functionalized nanopore (b) I–V curves recorded after PLL adsorption (red, square), after HEP (blue, circle) degraded by heparinase in presence (orange, triangle) or not (violet, triangle) of OSCS 0.1% weight (c) Rectification factor as a function of OSCS concentration (black, circle), in green and blue line are reported the two asymptotic values obtained without addition of OSCS and for non-degradated heparin. The results were obtained with a single conical nanopore d_{tip} = 12 nm and D_{base} = 540 nm. (For interpretation of the references to colour in this figure legend, the reader is referred to the Web version of this article.)

2018a).

Because the IRC depends on the degree of heparin degradation, we expected that the inhibition by OSCS can be also detected by nanopore. The first experiment was to compare the I–V curves after addition of heparine degraded by heparinase after 200 min incubation at 25 °C with and without 10% weight of OSCS (Fig. 5a). Without the inhibitor, the rectification factor decreases from 5.22 to 1.86 because the affinity of oligosaccharides with PLL is too weak to provide efficient charge compensation. In presence of OSCS the heparinase is inhibited and the HEP is less degraded. The long chains of heparin have a better affinity with the PLL inducing more efficient charge compensation characterized by a decrease of *Rf* until 0.9. The range of OSCS dose-response is reported on Figs. 5b and S7. The experiments conducted on two individual nanopores with tip diameter 12 nm and 36 nm show the same trend. The value *Rf* decreases with the OSCS concentration. For both nanopores the *Rf* is boundary between two asymptotic values the one obtained after heparin degradation without inhibitor and the one obtained after adsorption of non-degraded heparin. For all tested nanopores, the detection range where the *Rf* is dependent on the OSCS concentration is found from 0.1 to 10^{-4} w/w.

3.3. Stability and reproducibility of nanopore sensor

As mentioned in introduction, the main bottlenecks to use solid-state nanopore as sensor are their short lifetime and the difficulties to reproduce similar experiments several consecutive days without constraining experiments. We discuss now about the stability and the lifetime of our nanopore. For the heparin sensing, the experiments shown in Fig. 2 and S3 where 18 cycles performed in the same day are reported. For the dose response experiments (Fig. S5), 28 cycles was performed during two consecutive days. These results confirm that approach based on the reversible functionalization with PLL allows using the same nanopore for several experiments with a good reproducibility of results. The experiments about the OSCS sensing (Figs. 5b and S7) were performed during two consecutive days. In order to provide a clear proof of the nanopore stability, we show in Fig. 6, a series of HEP and HEP after degradation with by heparinase in presence of OSCS 1% detection experiments performed during 18 days. Between each experiment the nanopore was conserved in milliQ water. The result show that a good reproducility of results. Typically after each step the rectification factor stay comparable along the day. We notice also that after 18 days the nanopore is still working.

4. Conclusion

To sum up, the single nanopore sensor described herein can be used to detect easily a wide range of OSCS concentration contained in heparin sample. The detection limit about 0.01% weights that is less sensitive compared methods based on fluorescence but in the good range for the characterization of contaminated sample of heparin. In addition, our approach does not require the synthesis of fluorescent dyes, specific DNA ligands or nanoparticles nor expensive instrumentation. Indeed, the nanopore functionalization requires a couple of minutes and it is totally reversible which allows quantifying the OSCS after performed a calibration curve. It is also perfectly conceivable the integration of the nanopore inside a microfluidic device and use a miniaturized amplifier to build a portable system to analyze heparin sample. So, we could expect that this nanopore sensor will enhance the quality control chain of heparin allowing avoiding the risk of patients' death. Beside the detection of heparin contaminant, two other applications are possible with our nanopore: the characterization of enzymatic degradation of PE and the mechanism of PE layer formation. Globally, this study highlight that a conical nanopore simply functionalized with PLL is powerful for many applications from enzymology to controlling quality of drug.

Declaration of interests

The authors declare that they have no known competing financial interests or personal relationships that could have appeared to influence the work reported in this paper.

CRediT authorship contribution statement

Tianji Ma: Investigation, Validation, Formal analysis, Visualization. **Emmanuel Balanzat:** Resources. **Jean-Marc Janot:** Writing - review & editing. **Sébastien Balme:** Conceptualization, Methodology, Writing - original draft, Supervision.

Acknowledgement

Single tracks have been produced in GANIL (Caen, France) in the framework of an EMIR project. The authors thank Laurent Bacri from LAMBE university of Evry for the discussion about heparin contaminants.

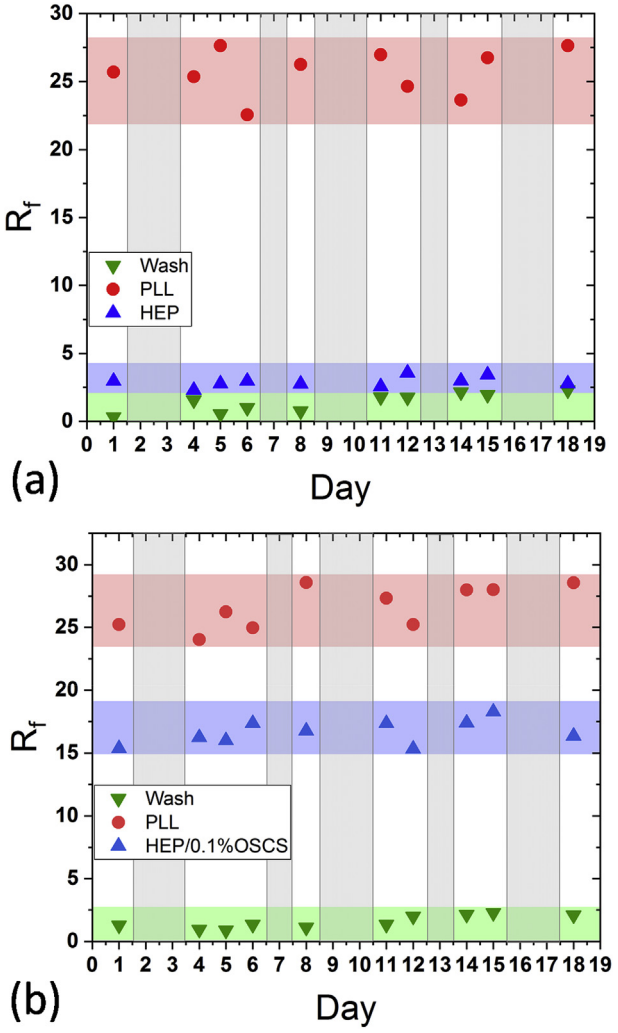

Fig. 6. Nanopore sensor stability and reproducibility: Rectification factor obtained for single nanopore, after PLL deposition (red, circle), and washing at pH 12 (green triangle) and (a) after HEP (blue, triangle) and (b) after HEP degradated by heparinase in presence of OSCS 0.1% weight (blue, triangle). The experiments were performed at different day on the same nanopore d_{tip} = 29 nm and D_{base} = 340 nm. The gray zone correspond to storage period without experiment (1 or 2 days). (For interpretation of the references to colour in this figure legend, the reader is referred to the Web version of this article.)

Appendix A. Supplementary data

Supplementary data to this article can be found online at https://doi.org/10.1016/j.bios.2019.05.005.

References

Ali, M., Ahmed, I., Ramirez, P., Nasir, S., Niemeyer, C.M., Mafe, S., Ensinger, W., 2016. Small 12, 2014–2021.
Ali, M., Nasir, S., Ensinger, W., 2015. 51, 3454–3457.
Ali, M., Neumann, R., Ensinger, W., 2010a. ACS Nano 4, 7267–7274.
Ali, M., Nguyen, Q.H., Neumann, R., Ensinger, W., 2010b. Chem. Commun. 46, 6690.
Beni, S., Limtiaco, J.F.K., Larive, C.K., 2011. Anal. Bioanal. Chem. 399, 527–539.
Dekker, C., 2007. Nat. Nanotechnol. 2, 209–215.
Ding, Y., Shi, L., Wei, H., 2015. Chem. Sci. 6, 6361–6366.
Fennouri, A., Daniel, R., Pastoriza-Gallego, M., Auvray, L., Pelta, J., Bacri, L., 2013. Anal. Chem. 85, 8488–8492.
Giamblanco, N., Coglitore, D., Gubbiotti, A., Ma, T., Balanzat, E., Janot, J.M., Chinappi, M., Balme, S., 2018a. Anal. Chem. 90, 12900–12908.
Giamblanco, N., Coglitore, D., Janot, J., Eugène, P., Charlot, B., Balme, S., 2018b. Sensor. Actuator. B Chem. 260, 736–745.
Guerrini, M., Zhang, Z., Shriver, Z., Naggi, A., Masuko, S., Langer, R., Casu, B., Linhardt, R.J., Torri, G., Sasisekharan, R., 2009. Proc. Natl. Acad. Sci. Unit. States Am. 106, 16956–16961.
Hu, Y., Guo, W., Ding, Y., Cheng, H., Wei, H., 2016. Biosens. Bioelectron. 86, 858–863.
Kalita, M., Balivada, S., Swarup, V.P., Mencio, C., Raman, K., Desai, U.R., Troyer, D., Kuberan, B., 2014. J. Am. Chem. Soc. 136, 554–557.
Karawdeniya, B.I., Bandara, Y.M.N.D.Y., Nichols, J.W., Chevalier, R.B., Dwyer, J.R., 2018. Nat. Commun. 9, 3278.
Kasianowicz, J.J., Brandin, E., Branton, D., Deamer, D.W., 1996. Proc. Natl. Acad. Sci. U.S.A. 93, 13770–13773.
Lepoitevin, M., Bechelany, M., Balanzat, E., Janot, J.-M., Balme, S., 2016a. Electrochim. Acta 211, 611–618.
Lepoitevin, M., Jamilloux, B., Bechelany, M., Balanzat, E., Janot, J.-M., Balme, S., 2016b. RSC Adv. 6, 32228–32233.
Lepoitevin, M., Ma, T., Bechelany, M., Janot, J.-M., Balme, S., 2017. Adv. Colloid Interface Sci. 250, 195–213.
Lepoitevin, M., Nguyen, G., Bechelany, M., Balanzat, E., Janot, J.-M., Balme, S., 2015. Chem. Commun. 51, 5994–5997.
Liu, Z., Xiao, Z., Masuko, S., Zhao, W., Sterner, E., Bansal, V., Fareed, J., Dordick, J., Zhang, F., Linhardt Robert, J.,R.J., 2011. Anal. Biochem. 408, 147–156.
Ma, T., Gaigalas, P., Lepoitevin, M., Plikusiene, I., Bechelany, M., Janot, J.M., Balanzat, E., Balme, S., 2018. Langmuir 34, 3405–3412.
Roman, J., Français, O., Jarroux, N., Patriarche, G., Pelta, J., Bacri, L., Le Pioufle, B., 2018. ACS Sensors under revision 3, 2129–2137.
Roman, J., Jarroux, N., Patriarche, G., Français, O., Pelta, J., Le Pioufle, B., Bacri, L., 2017. ACS Appl. Mater. Interfaces 9, 41634–41640.
Sasisekharan, R., Shriver, Z., 2009. Thromb. Haemostasis 102, 854–858.
Wang, Y.J., Lin, L., Zhang, X., Schultz, V., Zhang, F., Sun, J.Z., Linhardt, R.J., 2016. Anal. Biochem. 514, 48–54.